DOI: 10.1534/genetics.110.118406

Allele-Specific Suppressors of *lin-1(R175Opal)* Identify Functions of MOC-3 and DPH-3 in tRNA Modification Complexes in *Caenorhabditis elegans*

Sunhong Kim,*,[1,2] Wade Johnson,*,[1,3] Changchun Chen,[†] Aileen K. Sewell,* Anders S. Byström[†] and Min Han*,[4]

**Howard Hughes Medical Institute and Department of Molecular, Cellular and Developmental Biology, University of Colorado, Boulder, Colorado 80309 and* [†]*Department of Molecular Biology, University of Umeå, 901 87 Umeå, Sweden*

Manuscript received May 5, 2010
Accepted for publication May 8, 2010

ABSTRACT

The elongator (ELP) complex consisting of Elp1-6p has been indicated to play roles in multiple cellular processes. In yeast, the ELP complex has been shown to genetically interact with Uba4p/Urm1p and Kti11-13p for a function in tRNA modification. Through a *Caenorhabditis elegans* genetic suppressor screen and positional cloning, we discovered that loss-of-function mutations of *moc-3* and *dph-3*, orthologs of the yeast *UBA4* and *KTI11*, respectively, effectively suppress the Multivulva (Muv) phenotype of the *lin-1*(*e1275*, *R175Opal)* mutation. These mutations do not suppress the Muv phenotype caused by other *lin-1* alleles or by gain-of-function alleles of *ras* or *raf* that act upstream of *lin-1*. The suppression can also be reverted by RNA interference of *lin-1*. Furthermore, we showed that *dph-3(lf)* also suppressed the defect of *lin-1(e1275)* in promoting the expression of a downstream target (*egl-17*). These results indicate that suppression by the *moc-3* and *dph-3* mutations is due to the elevated activity of *lin-1(e1275)* itself rather than the altered activity of a factor downstream of *lin-1*. We further showed that loss-of-function mutations of *urm-1* and *elpc-1-4*, the worm counterparts of *URM1* and ELP complex components in yeast, also suppressed *lin-1(e1275)*. We also confirmed that *moc-3(lf)* and *dph-3(lf)* have defects in tRNA modifications as do the mutants of their yeast orthologs. These results, together with the observation of a likely readthrough product from a *lin-1(e1275)::gfp* fusion transgene indicate that the aberrant tRNA modification led to failed recognition of a premature stop codon in *lin-1(e1275)*. Our genetic data suggest that the functional interaction of *moc-3/urm-1* and *dph-3* with the ELP complex is an evolutionarily conserved mechanism involved in tRNA functions that are important for accurate translation.

THE MOCS3 protein has been shown to be involved in two unlinked cellular processes: molybdenum cofactor (Moco) synthesis and tRNA modification (Schwarz and Mendel 2006; Leidel *et al.* 2009). Moco is a cofactor of several essential metabolic enzymes (sulfite oxidase, xanthine dehydrogenase, aldehyde oxidase, and nitrate reductase), and, thus, the Moco synthesis pathway is conserved from bacteria to humans (Schwarz and Mendel 2006). In the Moco synthesis pathway, MOCS3 transfers a sulfur atom to the MOCS2B protein, and this sulfur atom is further transferred to the Moco precursor (supporting information, Figure S1A) (Schwarz and Mendel 2006). The structures of these two proteins and the sulfur transfer during Moco biosynthesis share significant similarities with the structures and functions of ubiquitin-activating enzymes, leading to the suggestion that the ubiquitin-dependent protein conjugation system may have evolved from the evolutionarily older Moco synthesis pathway (Schwarz and Mendel 2006).

MOCS3 has recently been found to have another ubiquitin-like partner, *URM1* (Ubiquitin-Related Modifier 1), in *Saccharomyces cerevisiae* (Furukawa *et al.* 2000; Goehring *et al.* 2003a,b; Rubio-Texeira 2007). Urm1p is conserved from yeast to humans (Furukawa *et al.* 2000) and known to be conjugated to proteins, as are other ubiquitin family members (Furukawa *et al.* 2000; Goehring *et al.* 2003a,b). A series of recent articles has demonstrated a novel function of the *URM1/UBA4* (MOCS3 yeast ortholog) pathway in the modification of cytosolic tRNAs (Huang *et al.* 2008; Nakai *et al.* 2008; Schlieker *et al.* 2008; Leidel *et al.* 2009; Noma *et al.* 2009). The oxygen atom in position 2 of the wobble

Supporting information is available online at http://www.genetics.org/cgi/content/full/genetics.110.118406/DC1.

[1]These authors contributed equally to this work.

[2]*Present address:* Korea Research Institute of Bioscience and Biotechnology, 685-2 Yangcheong-ri, Ochang-eup, Cheongwon-gun, Chungbuk, Republic of Korea 363-883.

[3]*Present address:* R&D Systems, Inc., 614 McKinley Place NE, Minneapolis, MN 55413.

[4]*Corresponding author:* Howard Hughes Medical Institute and Department of Molecular, Cellular, and Developmental Biology, Box 347, University of Colorado, Boulder, CO 80309-0347.
E-mail: humhan@colorado.edu

uridine, U_{34}, of several tRNAs is replaced with a sulfur atom, s^2U_{34}, requiring the Urm1p/Uba4p module (Figure S1B) (Huang *et al.* 2008; Nakai *et al.* 2008; Schlieker *et al.* 2008; Leidel *et al.* 2009; Noma *et al.* 2009). In addition, U_{34} is modified to a 5-methoxycarbonyl-methyl (mcm^5) or 5-carbamoylmethyluridine (ncm^5U), where an initial common step requires Kti11-13p proteins and the elongator protein (ELP) complex (Figure S1B) (Huang *et al.* 2005; Lu *et al.* 2005). The ELP complex had been indicated for roles in transcriptional elongation (Otero *et al.* 1999; Krogan and Greenblatt 2001; Kim *et al.* 2002), but it was also recently linked to tRNA modification (Huang *et al.* 2005; Lu *et al.* 2005; Esberg *et al.* 2006). It is noted that in the *elp* mutants of *S. cerevisiae*, lack of modification at position 5 will reduce thiolation at position 2 of U_{34} (Nakai *et al.* 2008; Leidel *et al.* 2009; Noma *et al.* 2009). A recent report, however, suggested that this hierarchy may not describe the situation in *Caenorhabditis elegans* (Chen *et al.* 2009). Furthermore, the Urm1p/Uba4p module and Kti11p have been shown to maintain Elp1p function by preventing post-translational modification of Elp1p (Fichtner *et al.* 2003).

C. elegans vulval development involves multiple steps during the four larval stages (L1–L4) (Sternberg 2005). The canonical RAS/RAF/MAPK pathway in *C. elegans* plays a critical role in inducing vulval differentiation during these stages (Sternberg and Han 1998; Sundaram 2005). Two key transcription factors have been shown to act downstream of MPK-1: LIN-1, an ETS family member protein, and LIN-31, a winged helix family member protein (Miller *et al.* 1993; Beitel *et al.* 1995; Kornfeld 1997). Loss of function of either transcription factor causes ectopic vulval induction [Multivulva (Muv) phenotype], indicating that these two genes act as negative regulators of vulval induction. A previous report also suggests that LIN-1 and LIN-31 form a functional heterodimer that represses vulval-specific functions (Tan *et al.* 1998). Upon activation of the RTK/RAS/MAPK pathway, MPK-1 phosphorylates both LIN-1 and LIN-31, breaking up the heterodimer and allowing for vulval induction (Figure S2). Currently, it is not clear how phosphorylation of LIN-1 triggers the cellular events related to vulval formation and what the direct regulatory targets of LIN-1 are.

In an attempt to identify factors that act downstream or with LIN-1 for its vulval function, we carried out genetic screens for mutations that can suppress the weak temperature-sensitive *lin-1* allele, *e1275*. We identified and cloned two genes defined by two of these suppressor mutations in *C. elegans*: *dph-3*, encoding a homolog to yeast *KTI11* and mammalian DPH3, and *moc-3*, encoding an ortholog of *UBA4*/MOCS3. We show that the suppressor effects of loss-of-function mutations (*lf*) in these two genes are highly specific to this single *lin-1* allele. Subsequent analysis revealed that these two evolutionarily conserved genes are not specifically involved in vulval cell differentiation, but are involved in tRNA modifications, the disruption of which leads to translational inaccuracy and the observed suppressor effects.

MATERIALS AND METHODS

Culture methods and strains: Maintenance, culturing, and genetic manipulations of *C. elegans* strains were carried out according to standard procedures (Brenner 1974) and conducted at 20°. The strains used or generated are as follows: *lin-1(e1275)*, *lin-1(n1047)*, *lin-1(e1275) unc-24(e138) dpy-20(e1282)*, *lin-1(e1275) moc-3(ku300)*, *lin-1(e1275) moc-3(tm3742)*, *lin-1(e1275) dph-3(ku305)*, *dph-3(ku432)*, *lin-1(e1275) dph-3(ku432)*, *lin-1(n1047) dph-3(ku432)*, *lin-1(n176) dph-3(ku432)*, *lin-1(n176) moc-3(tm3742)*, *let-60(sy130)*, *let-60(sy130) dph-3(ku432)*, *lin-45(gf)*, *lin-45(gf); moc-3(ku300)*, *lin-31(n301)*, *lin-31(n301); dph-3(ku432)*, *lin-31(n1053)*, *lin-31(n1053); moc-3(ku300)*, *elpc-3(ok2452)*, *lin-1(e1275); elpc-3(ok2452)*, *lin-1(n176); elpc-3(ok2452)*, *ayIs4[egl-17::GFP, dpy-20(+)]*, *Ex[pSK002(sur-5p::lin-1(e1275)::NLS::gfp)*, *psur-5p::DsRed, unc-119(+)]* (this article), and *kuIs76[sur-5p::gfp::lin-1(e1275)::flag, unc-119(+)]* (this article). Opal stop mutants used *dpy-5(e61)*, *lin-1(n176)*, and *lon-1(sp3)*. Information regarding each mutation can be found at http://www.wormbase.org.

Mutagenesis and phenotype scoring: *lin-1(e1275)* animals were mutagenized with 50 mM ethyl methanesulfonate (Brenner 1974). Mutagenized adults were individually transferred to a petri plate and allowed to lay eggs. The F_1 progeny were cloned to individual plates. The F_2 generation was then scored under a dissecting microscope for suppression of the Muv phenotype. Approximately 20,000 haploid genomes (10,000 F_1 plates) were screened, and 24 independent strains were isolated. A *moc-3* allele, *ku300*, and a *dph-3* allele, *ku305*, were mapped to LG IV. *moc-3(ku300)* and *dph-3(ku305)* were outcrossed more than five times. Muv percentage was scored under a dissecting scope as described previously (Ferguson and Horvitz 1985).

Genetic mapping and molecular cloning: *dph-3* and *moc-3* were mapped relative to the cloned markers *unc-24* and *dpy-20* on LG IV. The strains *lin-1(e1275) dph-3(ku305)/lin-1(e1275) unc-24(e138) dpy-20(e1282)*and *lin-1(e1275) moc-3(ku300)/lin-1(e1275) unc-24(e138) dpy-20(e1282)* were constructed, and a standard three-factor recombination analysis was performed. Further mapping was done by SNP analysis using a Bristol (N2)/Hawaii (CB4856) hybrid strain. The *lin-1(e1275)* strain was crossed to CB4856 10 times to generate a *lin-1* mutant strain with mostly Hawaii chromosomes. N2 *lin-1(e1275) unc-24(e138) ku305 dpy-20(e1282)/Hawaii lin-1(e1275)* and N2 *lin-1(e1275) unc-24(e138) ku300 dpy-20(e1282)/Hawaii lin-1(e1275)* were then constructed, and recombinants were isolated from them. Analysis of SNP sequence in the region pinpointed the genes to small genetic regions between cosmids W09C2 and K07F5 for *dph-3* and between cosmids C49H3 and T09A12 for *moc-3*.

Combination or individual cosmids in this region were injected at 1–10 ng/μl into *lin-1(e1275) dph-3(ku305)* or *lin-1(e1275) moc-3(ku300)* mutant animals to locate the gene activity that can rescue the mutant defect of *ku300* or *ku305* [*i.e.*, to recover the Muv phenotype associated with *lin-1(e1275)*]. The dominant marker SUR-5 TXN::GFP was co-injected at 50 ng/μl (Yochem *et al.* 1998). Cosmid ZK1251, as well as a subsequent subclone pWJ043 containing a 3-kb *Hin*dIII fragment and the gene K01H12.1, could rescue the *ku305* mutant phenotype. Cosmid F42G8, as well as an 8-kb *Sal*I fragment containing the coding sequence of F42G8.6, could rescue the *ku300* mutant phenotype.

Molecular analysis of the mutant lesion and RNA interference: To identify molecular lesions in the *ku300* and *ku305* alleles, the coding regions of the genomic DNA were PCR amplified, followed by sequence analysis. For RNA interference (RNAi) analysis, *moc-3*, *urm-1*, *dph-3*, *elpc-1*, *elpc-2*, *elpc-3*, and *elpc-4* cDNA were isolated from N2 worms and subcloned into the pPD129.36 RNAi feeding vector, and double-stranded-RNA-containing bacteria were fed to *lin-1(e1275); rrf-3(pk1426)* worms as described previously (Fire *et al.* 1998).

Targeted deletion mutation screen: N2 worms were mutagenized with UV-trimethyl psoralen (TMP) to create deletions (Yandell *et al.* 1994). These worms were processed according to a protocol described by R. Barstead (http://www.mutantfactory.ouhsc.edu/protocols.asp) and frozen into 1120 aliquots. The library was screened with 1° (primary) and 2° (secondary) reactions using two sets of primers. For the 1° reaction, a poison primer was also used. One-degree primers amplify 1581 bp, and their sequences are 5′-tcatccaaaggatccgggtcg and 3′-aaacaaaatcctcaagcttcc. The sequence of the poison primer is atgtcagttttccacgacgaag (beginning at the ATG of *dph-3*). The 2° primers amplify 680 bp, and their sequences are 5′-cccaacct ctctcgcccc and 3′-tttactcgcgaaacccgtatc.

Double-mutant analysis: Double mutants in Tables 1–3 were constructed and analyzed by standard genetic method. To analyze the suppression effect of *moc-3(ku300)* on *lin-1(n303)*, we generated *lin-1(n303)/moc-3(ku300) dpy-20(e1282)* animals and identified 23 L4 animals that were homozygous for both the *lin-1* and *dpy-20* alleles and derived from at least 12 independent recombination events. All of these animals became severely Muv, and all but three were lethal as adults without any progeny. Since the *moc-3* gene is located much closer to *dpy-20* (1.6 μm) than to *lin-1* (12.3 μm), most of these recombinants are expected to be homozygous for *moc-3(ku300)*, suggesting that the *moc-3* allele failed to suppress the Muv phenotype of the *lin-1* allele and that the double mutants were lethal.

Quantitative PCR: RNAs of mixed-stage worms were isolated by Trizol (Sigma, St. Louis) extraction. Quantitative PCR (qPCR) was performed on the Rotor-gene RG-3000 (QIAGEN, Germantown, MD). The primers used were *rpl-26* (5′-atgaaggt caatccgttcgt and 3′-aggacacgtccagtgtttcc; 209 bp) and *lin-1* (5′-ccacatttggcgtcccagtcac and 3′-tttgtggcctggaatgcggag; 152 bp). Amplification was done with SYBR Green JumpStart Taq Ready Mix (Sigma).

Transgenic line: *unc-119(ed3);him-5(e1467)* adults were injected with two different mixes: (1) 5 ng/μl pSK002, 30 ng/μl p*sur-5p*::DsRed, 50 ng/μl unc-119(+), 50 ng/μl pBluescript SK and (2) 5 ng/μl pSK016, 50 ng/μl unc-119(+), 50 ng/μl pBluescript SK. The latter established a stable extrachromosomal array line and was subjected to UV irradiation for the generation of the genomic integration line according to the modified version of the original protocol from S. Mitani (http://www.faculty.ucr.edu/~mmaduro/int.html). Briefly, 200–300 L4 worms were washed with M9 buffer several times to remove the residual bacteria. Then the worms were put on NGM plates without bacteria and irradiated with 300 J/m^2 of 254 nm UV using Stratalinker 2400 (Stratagene, La Jolla, CA). L4 worms were subsequently transferred to an OP50 plate at 10 animals/plate and incubated for 7–10 days until the animals on the plates were starved out. Two days after moving the animals to a new OP50 plate, the candidate integrant animals were singled to another plate to see if the progeny were all integrants. The resulting integration line was outcrossed three times against *unc-119(ed3);him-5(e1467)*. To confirm the expression of pSK016, we performed Western blot from mixed-stage worms according to the standard procedure.

TABLE 1

Allele-specific suppression of the Muv phenotype of *lin-1(e1275)* by *moc-3(lf)* and *dph-3(lf)*

Genotype	% multivulva (*n*)[a]
lin-1(e1275)	81.9 (191)
dph-3(ku305)	0.0 (100)
lin-1(e1275) dph-3(ku305)	1.2 (169)
dph-3(ku432)	1.0 (100)
lin-1(e1275) dph-3(ku432)	7.6 (131)
moc-3(ku300)	0.0 (100)
lin-1(e1275) moc-3(ku300)	1.6 (122)
lin-1(e1275) moc-3(tm3742)	6.6 (333)
lin-1(n176)	100 (100)
lin-1(n1047)	100 (100)
lin-1(n1047) dph-3(ku432)	100 (100)
lin-1(n176) dph-3(ku432)	100 (100)
lin-1(n176) moc-3(tm3742)	100 (50)

[a] Percentage of Muv animals at adult stage. *n*, the number of animals scored.

tRNA isolation and HPLC analysis: tRNAs from *C. elegans* were extracted and analyzed by HPLC as described previously (Chen *et al.* 2009).

RESULTS

***moc-3(lf)* and *dph-3(lf)* mutations suppress the Muv phenotype of a *lin-1* temperature-sensitive mutation:** We carried out a genetic screen for mutations that could suppress the Muv phenotype of a partial *lf* allele of *lin-1*, *e1275*. *lin-1*(*e1275*) has a nonsense mutation that causes variable Muv phenotypes at different temperatures (Beitel *et al.* 1995). We screened 20,000 mutagenized *lin-1(e1275)* haploid genomes at 20° and isolated 24 suppressors. Two of these suppressors, *ku300* and *ku305*, reduced the Muv phenotype from 81.9% to 1.6% and 1.2%, respectively, at 20° (Table 1). After molecular cloning of the genes defined by these two mutations (see below), we named the gene defined by the *ku300* allele as *moc-3* (**MOC**o synthesis pathway gene **3**, F42G8.6), and the gene defined by the *ku305* allele as *dph-3* (homolog of mammalian **DPH3** proteins).

While the recessive nature of *ku300* and *ku305* suggests that they may be *lf* mutations, the molecular lesions (see below) do not provide the basis for such a conclusion. Large-deletion mutations of both genes suppressed the Muv phenotype of *lin-1(e1275)* to a similar extent as the two alleles isolated in the suppressor screen (Table 1), indicating that the suppressors are indeed *lf* mutations. The *dph-3* deletion allele, *ku432*, was isolated by screening a UV-TMP-generated deletion mutation library (Figure 1A). The *moc-3*(*tm3742*) deletion allele was obtained from the National Bioresource Project (Mitani lab, Tokyo Women"s Medical University) (Figure 2A). Furthermore, the *lf* nature is supported by the fact that RNAi of *moc-3* and *dph-3* also suppressed the Muv phenotype of *lin-1(e1275)* (Table 2).

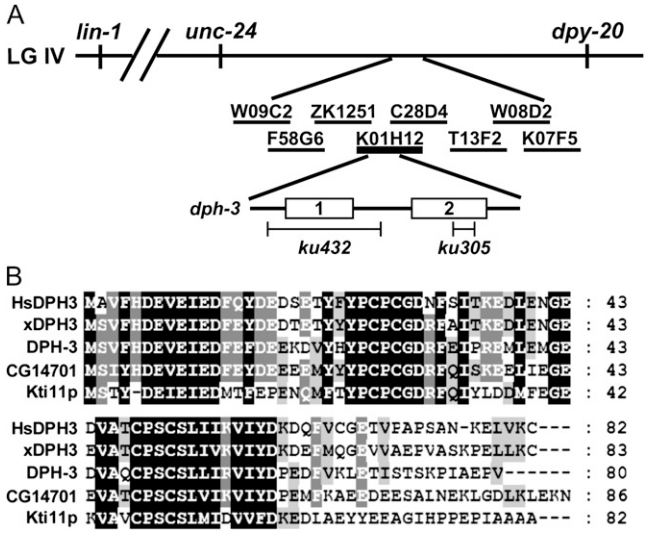

FIGURE 1.—Molecular cloning and sequence analysis of *dph-3* defined by a *lin-1(e1275)* suppressor mutation. (A) Cartoon of the *dph-3* location relative to mapping marker and rescuing DNA clones and regions uncovered by the two deletion mutations. (B) Protein alignment of DPH-3 and its orthologs in other representative eukaryotes. The orthologs are *Homo sapiens* (HsDPH3), *Xenopus laevis* (xDPH3), *Drosophila melanogaster* (CG14701), and *S. cerevisiae* (Kti11p). Alignment of multiple protein sequences was produced by Clustalw (http://align.genome.jp/) and edited manually by using GENEDOC (http://www.nrbsc.org/gfx/genedoc/).

***moc-3(lf)* and *dph-3(lf)* mutations do not suppress the Muv phenotype caused by other *lin-1* alleles or by mutations in other components in the vulval induction pathway:** To investigate the mechanism of the observed suppression, we tested whether the suppression by the *moc-3* and *dph-3* alleles is specific to the *lin-1(e1275)* allele. We generated double mutants combining the *moc-3(lf)* or *dph-3(lf)* allele with three other stronger *lin-1(lf)* alleles: *lin-1(n176)*, a premature opal stop codon at R255; *lin-1(n1047)*, an Y126F missense mutation; and *lin-1(n303)*, a R121K missense mutation (BEITEL *et al.* 1995). Surprisingly, *lin-1(n176)* and *lin-1(n1047)* were not suppressed by *moc-3(lf)* or *dph-3(lf)* (Table 1), and *lin-1(n303)* also appeared not to be suppressed by *moc-3(lf)* (data not shown; MATERIALS AND METHODS), suggesting that the suppression of *lin-1(e1275)* by *moc-3(lf)* and *dph-3(lf)* depended on either the relatively weak penetrance of the mutant phenotype or an unknown property of the *e1275* allele.

We next tested whether *moc-3(lf)* and *dph-3(lf)* genetically interact with mutations in *ras* and *raf* genes that also cause an incompletely penetrant Muv phenotype like *lin-1(e1275)* (BEITEL *et al.* 1990; HAN and STERNBERG 1990; YODER *et al.* 2004). Strikingly, no suppression was observed in *dph-3(ku432) let-60/ras(sy130gf)*, *lin-45/raf(gf); moc-3(ku300)*, or *lin-45/raf(gf); dph-3(ku432)* (Table 3). Furthermore, *moc-3(lf)* and *dph-3(lf)* did not suppress the Muv phenotype of a *lin-31(lf)* allele, which also acts in the Ras/MAPK pathway as described (Table 3). Since the Muv phenotypes of the *ras*, *raf*, and *lin-31* alleles are not stronger than the *lin-1(e1275)* allele, these results indicate that *moc-3(lf)* and *dph-3(lf)* specifically alter the gene activity of *lin-1(e1275)* rather than reduce the output of the signaling pathway.

To further support a role for *moc-3(lf)* and *dph-3(lf)* in elevating *lin-1(e1275)* gene activity that leads to the suppression, we applied *lin-1* RNAi on *lin-1(e1275) moc-3(ku300)* and *lin-1(e1275) dph-3(ku432)* strains and found that the treatment restored the Muv phenotype in both strains (Table S1).

***dph-3* encodes a conserved protein homologous to *DPH3/KTI11*:** We mapped *dph-3(ku305)* using genetic and SNP markers and cloned it by microinjection transformation (MATERIALS AND METHODS). Sequencing DNA from *lin-1(e1275) dph-3(ku305)* worms revealed a 28-bp deletion within exon 2 of the predicted open reading frame K01H12.1 (Figure 1A). This deletion eliminates the 19 C-terminal amino acids and replaces them with 13 alternate amino acids. RT–PCR data indicated that this altered transcript was produced in *ku305* worms (data not shown). This mutation did not remove any of the conserved cysteine residues necessary for Zn^{2+} binding (SUN *et al.* 2005). We also determined that *ku432* contains a 298-bp deletion that eliminated 57 bp of the promoter, the first exon (132 bp), and 109 bp of intronic DNA (Figure 1A). Given the small size of the gene, this deletion almost certainly eliminates the gene function (null allele). BLAST search indicated that *dph-3* encodes an 80-amino-acid protein that is highly conserved from yeast to humans (Figure 1B). The *S. cerevisiae* homolog, Kti11p, is associated with the ELP/Toxin Target (TOT) protein complex that has been proposed to be involved in transcriptional elongation as described above (FICHTNER and SCHAFFRATH 2002) (see below for additional discussion). Kti11p has been thought to function within the elongator complex by inhibiting the post-translational modification of Elp1p (FICHTNER *et al.* 2003). In yeast and mammalian cells, *KTI11* was independently identified as *DPH3/DESR1* (LIU and LEPPLA 2003; LIU *et al.* 2004). DPH3 is a component of the diphthamide synthesis protein complex that was suggested to play a role in a certain translation processes and has been shown to be essential in mouse development (LIU *et al.* 2006).

***moc-3* encodes a sulfur transferase in the MOCO synthesis pathway:** *moc-3(ku300)* was also genetically mapped and identified to be a candidate allele of *moc-3 (F42G8.6)* through microinjection transformation. Sequencing DNA from *lin-1(e1275) moc-3(ku300)* worms revealed a G-to-A point mutation within the coding region, which is expected to result in a D310N missense mutation in the Rhodanese domain that is important for the sulfur transferase activity of this family of proteins (Figure 2). Protein sequence alignment of *moc-3* orthologs showed that D310 is highly conserved in eukaryotes, implicating a critical role of this amino acid

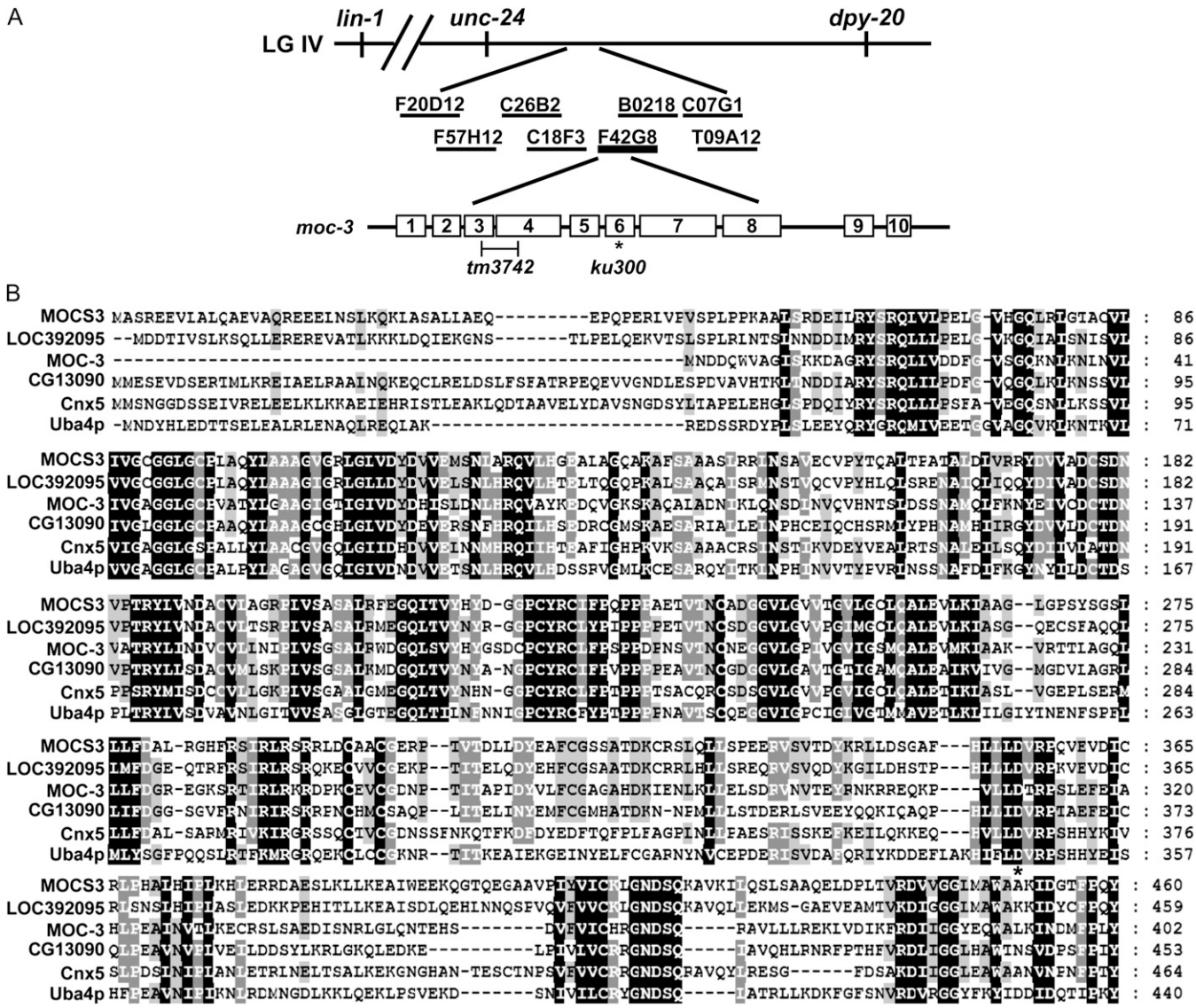

FIGURE 2.—Molecular cloning and sequence analysis of *moc-3* defined by a *lin-1(e1275)* suppressor. (A) Cartoon of the *moc-3* location relative to mapping markers and rescuing DNAs and regions uncovered by deletion mutations. The asterisk indicates the site of *ku300* mutation. (B) Alignment of MOC-3 and its orthologs in other species. The orthologs were chosen from the representative eukaryotic species of *H. sapiens* (MOCS3), *Danio rerio* (LOC393095), *D. melanogaster* (CG13090), *Arabidopsis thaliana* (Cnx5), and *S. cerevisiae* (UBA4). Alignment of multiple protein sequences was produced by Clustalw (http://align.genome.jp/) and edited manually by using GENEDOC (http://www.nrbsc.org/gfx/genedoc/).

in MOC-3 function (Figure 2B). The *tm3742* deletion allele of *moc-3* (Mitani Lab) lacks 321 C-terminal amino acids after V81, with an addition of 24 unrelated amino acids (Figure 2A), strongly suggesting that it is also a null allele. As *ku300* showed similar suppression of *lin-1 (e1275)* to *tm3742*, we concluded that the D310N mutation of *ku300* also abrogated the function of MOC-3 protein.

***dph-3(lf)* also suppresses the defect of *lin-1(e1275)* in promoting *egl-17* expression:** In addition to the negative role in repressing vulval induction, LIN-1 also has a positive role in vulval development, as it is required for the expression of *egl-17* in vulval cells (TIENSUU *et al.* 2005). An *egl-17::gfp* reporter is expressed in P6.p during the first two rounds of vulval cell division, and then its expression shifts to descendants of P5.p and P7.p (Figure 3, A, D, and G) (BURDINE *et al.* 1998; CUI and HAN 2003). In *lin-1(e1275)* worms, *egl-17::gfp* was not expressed in P6.p (Figure 3, B, E, and H), whereas, in *lin-1(e1275) dph-3(ku432)* worms, *egl-17::gfp* expression in P6.p was restored to wild type (Figure 3, C, F, and I). The simplest interpretation of these results is that there was an increase in LIN-1 activity in the presence of the *dph-3(ku432)* mutation.

Mutating ELP complex components also suppressed the Muv phenotype of *lin-1(e1275)*: As we mentioned above, the ELP complex has been shown to physically or functionally interact with Kti11p, a yeast ortholog of DPH-3, and Uba4p, a yeast counterpart of MOC-3 (FICHTNER *et al.* 2003). The yeast ELP complex is composed of six genes (*ELP1–6*) (KROGAN and GREENBLATT

TABLE 2

Suppression of *lin-1(e1275)* Muv phenotype by loss-of-function of *urm-1* and genes of the Elongator complex

Genotype	% multivulva (*n*)[a]
GFP RNAi	85 (93)
dph-3 RNAi	16 (101)
moc-3 RNAi	21 (185)
urm-1 RNAi	50 (192)
elpc-1(Y110A7A.16) RNAi	27 (195)
elpc-2(Y111B2A.17) RNAi	44 (207)
elpc-3(ZK863.3) RNAi	12 (82)
elpc-4(C26B2.6) RNAi	42 (210)
lin-1(e1275);elpc-3(ok2452)	12 (150)
lin-1(n176);elpc-3(ok2452)	100 (69)

[a] L4 worms of *lin-1(e1275);rrf-3(pk1426)* were placed on RNAi plate and Muv phenotype of F_1 were scored. *n*, the number of animals scored.

TABLE 3

***moc-3(lf)* and *dph-3(lf)* did not block Ras/MAPK pathway**

Genotype	% multivulva (*n*)[a]
let-60(sy130)	57 (100)
let-60(sy130) dph-3(ku432)	65 (100)
lin-45(gf)	48 (100)
lin-45(gf); moc-3(ku300)	53 (100)
lin-45(gf); dph-3(ku432)	55 (100)
lin-31(n301)	78 (100)
lin-31(n301); dph-3(ku432)	83 (100)
lin-31(n1053)	76 (100)
lin-31(n1053); moc-3(ku300)	71 (100)

[a] Percentage of Muv animals at adult stage. *n*, the number of animals scored.

2001; Winkler *et al.* 2001) and, among them, *ELP1–4* are conserved in *C. elegans* on the basis of protein sequence homology. These worm genes have thus been named as *elpc-1*, *elpc-2*, *elpc-3*, and *elpc-4*. *elpc-1* and *elpc-3* have also been recently shown to be functionally conserved with respect to the tRNA modification activity in *C. elegans* (Chen *et al.* 2009). To determine if the functions of *moc-3* and *dph-3*, indicated by the ability of their mutations to suppress *lin-1(e1275)*, reflect the functions of the ELP protein complex, we performed RNAi analysis on the *C. elegans* orthologs of the subunits of the yeast ELP complex. RNAi of *elpc-1*, *-2*, *-3*, and *-4* was able to significantly suppress the Muv phenotype (12–44% Muv; Table 2) of *lin-1(e1275)*, which was comparable to the effect of RNAi on *moc-3* and *dph-3* (Table 2). In addition, a null allele of *elpc-3*, *ok2452*, also showed strong suppression of the Muv phenotype of *lin-1(e1275)* (Table 2). By contrast, *lin-1(n176); elpc-3(ok2452)* still displayed the fully penetrant Muv phenotype, as did *lin-1(n176)* alone (Table 2). The allele-specific suppression by *elpc-3(ok2452)* suggests that the functional interactions of the ELP complex with *moc-3* and *dph-3* are evolutionarily conserved. We also analyzed the RNAi effects of the *moc-3*, *urm-1*, and *dph-3* genes on *lin-1(e1275); elpc-3(ok2452)* to further examine the functional relationship between *elpc-3* and the other three genes. As shown in Table S2, RNAi of any of the three genes did not enhance the suppression of the Muv phenotype by *elpc-3(ok2452)*, supporting the theory that *moc-3*, *urm-1*, *dph-3*, and the ELP complex act in the same pathway for the function related to suppression.

***moc-3* and *dph-3* mutations do not increase the level of *lin-1(e1275)* mRNA:** Given that the ELP complex has been known to regulate transcriptional elongation as mentioned earlier, a possible hypothesis is that *moc-3* and *dph-3* regulate the transcription of *lin-1*. To test this possibility, we performed quantitative RT–PCR to measure the *lin-1* transcript level. The mRNA level of *lin-1* in the *lin-1(e1275)* background was ~50% of the wild-type level, consistent with the theory that nonsense-mediated mRNA decay is involved in degrading the *lin-1(e1275)* transcript (Figure 4, bars 1 and 2). Neither *lin-1(e1275) moc-3(ku300)* nor *lin-1(e1275) dph-3(ku432)*, however, showed a statistically significant difference in *lin-1* mRNA level compared to *lin-1(e1275)* alone (Figure 4, bars 3 and 4; $P > 0.05$). These results suggested that *moc-3* and *dph-3* are unlikely to play a significant role in *lin-1* transcriptional regulation or mRNA stability.

tRNA modification leading to stop-codon read-through is the likely mechanism for suppression of *lin-1(e1275)* by mutations in *moc-3*, *dph-3*, and the ELP complex: As we described above, Uba4p has a tRNA modification function with its partner, Urm1p (Huang *et al.* 2008; Nakai *et al.* 2008; Schlieker *et al.* 2008; Leidel *et al.* 2009; Noma *et al.* 2009). To confirm that MOC-3 and DPH-3 are involved in tRNA modification as their yeast counterparts, we examined wobble uridine tRNA modification by HPLC analysis. Whereas the mcm^5s^2U nucleoside at the wobble position of tRNA was seen as a prominent peak in samples from N2 and *lin-1(e1275)* control worms, this peak was missing in *moc-3(lf)* and *dph-3(lf)* mutants (Figure 5 and Table S3). Furthermore, in *dph-3(lf)* background, the s^2U nucleoside arose due to the failure of the addition of the mcm^5 side chain (Table S3). These data confirm that, like their yeast orthologs, DPH-3 and MOC-3 are required for the formation of the mcm^5 and s^2 side chains, respectively. For an unknown reason, the modified wobble uridine was observed to be slightly less abundant in *lin-1(e1275)* mutants than in wild type (Figure 5 and Table S3). Given that the formation of this modified nucleoside has been shown to be complicated, involving multiple enzymatic activities in yeast (Huang *et al.* 2008), this difference may reflect an unknown LIN-1 function in the Elongator complex and thereby the formation of this nucleoside.

To determine whether the suppression of *lin-1(e1275)* by *moc-3* is mediated by this conserved Uba4p/Urm1p module, *urm-1*(RNAi) of *lin-1(e1275)* was tested. In-

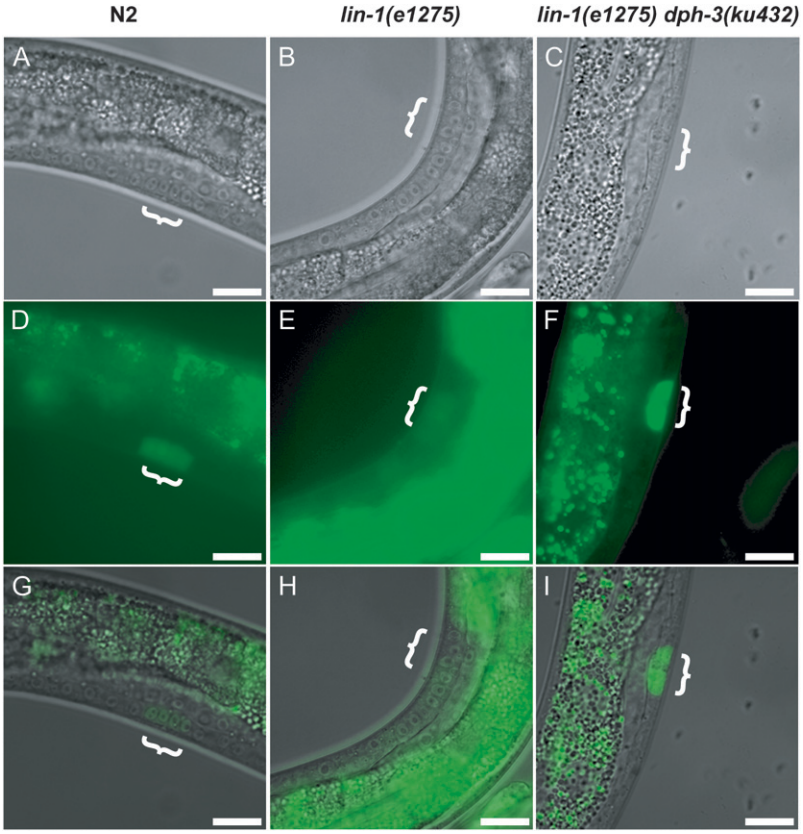

Figure 3.—The reduced expression of the *egl-17::GFP* reporter in *lin-1(e1275)* was restored by *dph-3(ku432)*. Nomarski (A, B, and C), GFP fluorescence (D, E, and F), and merged (G, H, and I) images of L3 larvae of the genotypes indicated. Exposure time of E and H was about 5 times longer than others to show the reduced expression of the reporter gene. White braces indicate the progeny of P6.p that express *egl-17::GFP* in wild-type animals but not in *lin-1(lf)* mutants (Burdine *et al.* 1998). Bars, 20 μm.

terestingly, RNAi of *urm-1* significantly suppressed the Muv phenotype of *lin-1(e1275)* (Table 2). This result led us to hypothesize that a tRNA modification defect in *moc-3(lf)* and *dph-3(lf)* animals leads to an increase in translational readthrough of the opal stop codon in *lin-1 (e1275)* transcripts.

This readthrough hypothesis is also supported by additional circumstantial evidence. As described earlier, the inability of the *moc-3* and *dph-3* mutations to suppress the Muv phenotype of other *lin-1(lf)* mutants and *ras/raf gf* mutants, as well as their loss of suppression by *lin-1* (RNAi), indicates that *moc-3(lf)* and *dph-3(lf)* alter the activity of *lin-1* itself. We have also shown that the mRNA level of *lin-1* is not raised in the *moc-3* or *dph-3* mutants. Causing readthrough of the opal stop codon of the *lin-1 (e1275)* allele appears to be the most logical explanation because the truncated protein is highly unlikely to be functional. The truncation is expected to delete the LIN-1 transactivation domain, presumably disrupting the basic function of this transcription factor. This assumption is also consistent with the fact that the *lin-1(n176)* allele, which is characterized as a strong *lf* or null allele on the basis of its completely penetrant phenotype, contains a premature stop (R255Opal) that is predicted to produce a truncated protein larger than the *e1275* truncated protein (R175Opal).

To observe the readthrough protein product from the *lin-1(e1275 R175Opal)* allele, we generated transgenic worms containing a *sur-5p::lin-1(e1275)::gfp* fusion gene (Figure 6A) and a *sur-5::DsRed* marker on the same extrachromosomal array. The *sur-5* promoter drives near-ubiquitous expression in *C. elegans* (Yochem *et al.* 1998), with GFP expression in this strain expected to depend on the translation reading through the premature opal stop codon. We observed prominent GFP expression in a fraction of cells in the *moc-3(ku300)* mutant animals but not in the wild-type background (Figure 6B). The GFP expression was not detectable in a number of cell types including vulval cells, even in *moc-3(ku300)*, likely due to a low-level expression of the transgene in these cells. We have not been able to directly detect the readthrough protein product using antibodies from commercial sources, nor those generated in our own lab; all immunochemical tests failed to detect LIN-1 protein on a Western blot from whole-worm extracts (data not shown). We also generated an integrated transgenic line, *kuIs76*, which ubiquitously expressed GFP-LIN-1(*e1275*)-FLAG proteins under the *sur-5* promoter (Figure S3) (Gu *et al.* 1998). *kuIs76* worms showed a high level of stable GFP expression throughout all stages and in most tissues, including the vulva (Figure S3B). We were also able to detect the truncated LIN-1(*e1275*) protein from mixed-stage worm lysates by Western blot (Figure S3C). However, we failed to detect the full-length GFP-LIN-1-FLAG proteins expressed from this transgene in the *moc-3(lf)* or *dph-3(lf)* background by Western blot following immunoprecipitation using anti-GFP or FLAG antibodies. A likely explanation

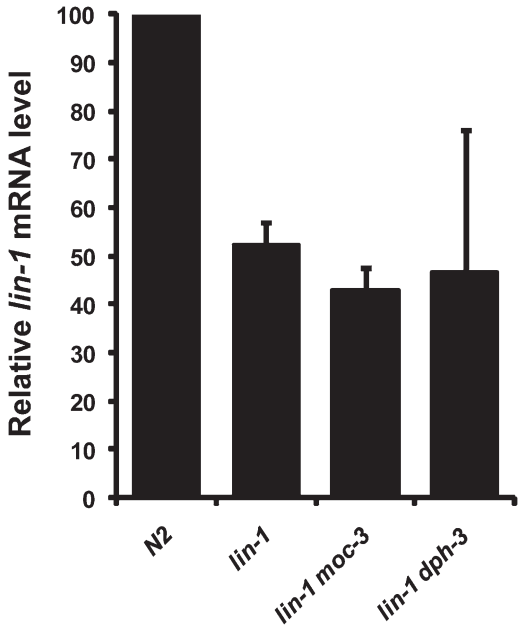

FIGURE 4.—*lin-1* mRNA level was not affected by mutating either *dph-3* or *moc-3*. Bar graph indicates the results of qRT–PCR analysis of mRNA levels of *lin-1* in the strains listed. *rpl-26* was used as an internal control during the qRT–PCR experiments. Error bar indicates ±SD. Statistical analysis is described in the RESULTS.

for this outcome is that the readthrough product is only a very small fraction of the total LIN-1 protein and/or the readthrough occurred in only a small fraction of tissues. Presumably, this low-level expression is sufficient for its function in vulval cells but eluded detection by Western blot. To test if there is a small amount of LIN-1 full-length protein from *kuIs76*, we generated a series of double or triple mutants as depicted in Table 4. We found that *kuIs76* significantly suppressed the fully penetrant Muv phenotype of *lin-1 (n176) moc-3(tm3742)* and *lin-1(n176) dph-3(ku432)* (Table 4). Furthermore, the Muv phenotype of *lin-1(n176)* was slightly suppressed by *kuIs76* alone (Table 4), consistent with the incomplete penetrance phenotype and temperature-sensitive nature of *lin-1(e1275)*. These genetic data are consistent with the theory that the opal stop codon of *e1275* causes leaky translation and thus favors the hypothesis that the defects in tRNA modification in *moc-3(lf)* or *dph-3(lf)* mutants lead to the translational readthrough of *lin-1(e1275)*.

DISCUSSION

We have identified novel mutant phenotypes of *moc-3* and *dph-3* genes in suppressing the developmental defects of a temperature-sensitive allele (*e1275*) of *lin-1* that encodes an ETS domain transcription factor. The *lin-1(e1275)* allele harbors a premature opal stop codon that is expected to produce a truncated LIN-1 protein without its regulatory domain (BEITEL *et al.* 1995). Results of a series of genetic analyses provide strong evidence that the suppression conferred by *moc-3* and *dph-3* mutations is due to a specific increase in the activity of the *lin-1(e1275)* mutant gene. We also provide evidence for the idea that aberrant tRNA modification leads to failed recognition of the premature stop codon in *lin-1(e1275)*. Our results suggest that the functional interaction of *moc-3/urm-1* and *dph-3* with the ELP complex is an evolutionarily conserved mechanism involved in tRNA functions that are important for accurate translation.

Our proposal that the *moc-3* and *dph-3* mutations affect LIN-1 (e1275) protein translation via tRNA modification defects is based on the following pieces of data. First, *moc-3(lf)* and *dph-3(lf)* each suppresses the Muv phenotype of the opal allele *e1275*, but not of other *lin-1(lf)* alleles (Table 1). They also failed to suppress the incompletely penetrant Muv phenotypes of gain-of-function alleles of *ras* and *raf* that act upstream of LIN-1 in the vulval induction pathway (Table 3). Therefore, loss of *moc-3* or *dph-3* function may simply result in an increase in the level of functional LIN-1 protein. This conclusion is supported by *lin-1* RNAi data showing a reversed suppression of the Muv phenotype in *lin-1(e1275) moc-3(ku300)* and *lin-1(e1275) dph-3(ku432)* (Table S1). Second, the decreased expression of *egl-17::GFP* in the *lin-1(e1275)* mutant has been restored by the *dph-3(lf)* mutation (Figure 3). Because promoting *egl-17* expression represents a positive role of LIN-1 as opposed to its negative role on vulval induction reflected by the Muv phenotype of the *lin-1(lf)* alleles, this result also supports the theory that *dph-3(lf)* specifically elevates *lin-1(e1275)* gene activity. Third, the overexpressed GFP-LIN-1 (e1275) protein did not substantially suppress the Muv phenotype of *lin-1(e1275)* mutants under conditions where both *moc-3* and *dph-3* are functional (Table 4). This supports the idea that the truncated LIN-1 (e1275) protein has little or no intrinsic activity and that suppression conferred by the mutants of *moc-3* and *dph-3* is due to increased readthrough of the opal stop codon in *lin-1(e1275)* mRNA (Table 4). The notion that the truncated LIN-1 protein produced by the *e1275* allele lacks the wild-type function is also consistent with the fact that the strong loss-of-function *lin-1(n176, R255Opal)* allele is expected to produce a protein longer than that from *lin-1(e1275, R175Opal)*. Fourth, RNAi or deletion mutants of components of the recently discovered tRNA modification modules, *urm-1* (LEIDEL *et al.* 2009) and the ELP complex (CHEN *et al.* 2009), also displayed similar suppression of *lin-1(e1275)* as did *moc-3* and *dph-3* mutations (Table 2). Notably, a recent study proved that *elpc-1* and *elpc-3* play an evolutionarily conserved role in tRNA modification and that their mutants displayed specific neurological and developmental defects (CHEN *et al.* 2009), suggesting that tRNA modification defects appear to be restricted to certain specific cellular processes. Fifth, RNAi of *moc-3*, *dph-3*,

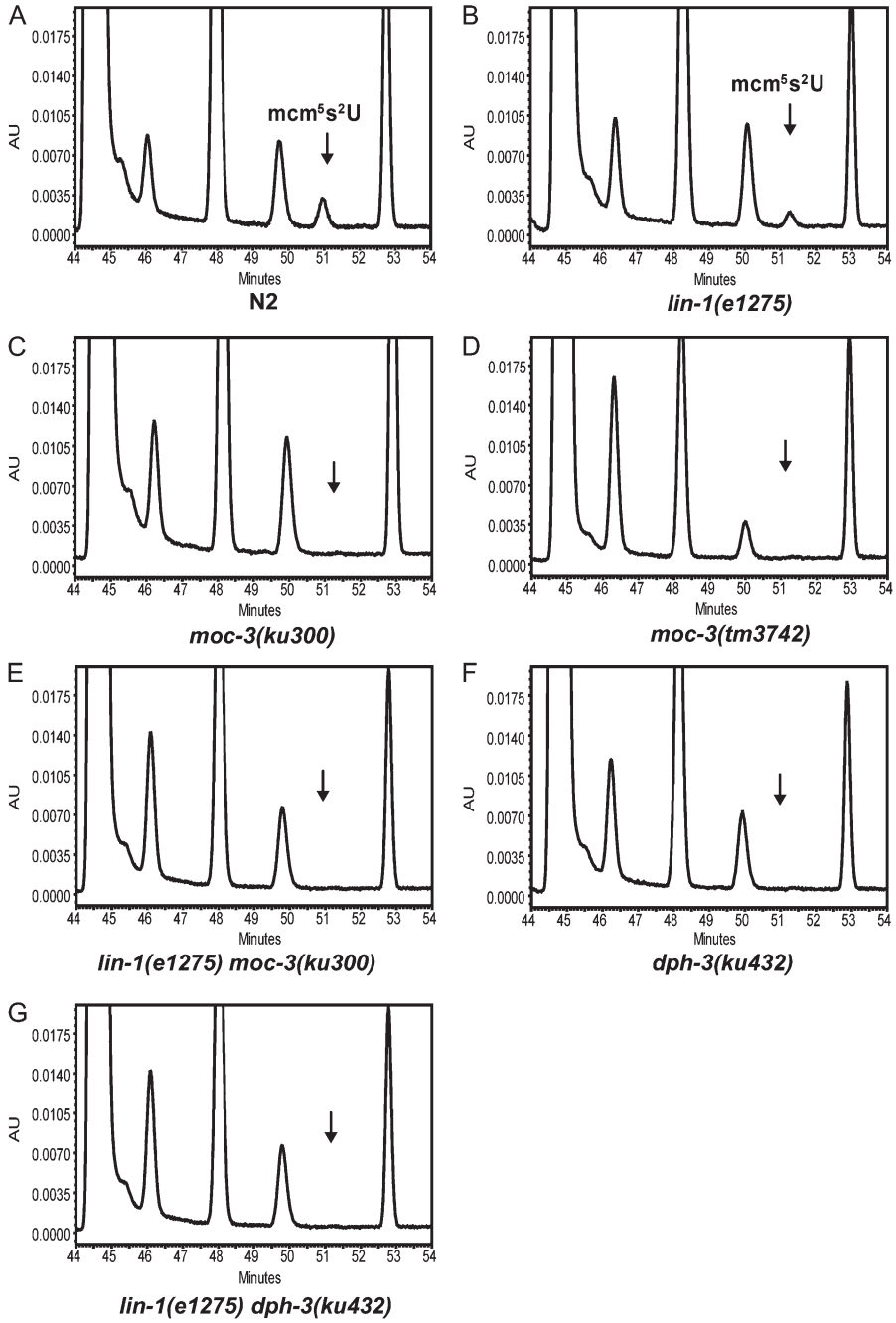

FIGURE 5.—*moc*-3 and *dph-3* are required for the formation of the wobble uridine nucleoside mcm^{5}s^{2}U. Chromatograms constructed on the basis of HPLC analysis of modified tRNA nucleosides from strains of indicated genotypes are shown. Chromatograms were monitored at 254 nm, and only the graphs between retention time 44 and 54 are shown. The arrows in A–G indicate the expected retention time of mcm^{5}s^{2}U.

and *urm-1* did not enhance the suppression of the Muv phenotype of *lin-1(e1275)* by *elpc-3(ok2452)*, suggesting that they belong to the same biochemical pathway (Table S2). Notably, the Moco synthesis pathway, another functional partner of *moc-3*, did not affect the Muv phenotype of *lin-1(e1275)* via RNAi or null mutation (data not shown), indicating that the tRNA modification function of the *moc-3/urm-1* module, not the Moco synthesis function, is responsible for this suppression ability. Sixth, we were able to detect the expression of a GFP fusion protein that is expected to be the readthrough translation product from a *lin-1(e1275)::gfp* transgene in the *moc-3(ku300)* mutants (Figure 6). Finally, biochemical analysis indicates that *moc-3* and *dph-3* play roles in tRNA modification; the mcm^{5}s^{2}U species of the tRNA wobble uridine were missing in samples from *moc-3(lf)* and *dph-3(lf)* mutants. While these data strongly support the idea that defects in tRNA modification lead to increased readthrough of the opal stop codon in *lin-1(e1275)*, we have not been able to directly detect the readthrough protein product by biochemical methods (see RESULTS).

Studies in yeast indicate that the ELP complex interacts with the C-terminal tail of RNA polymerase II (RNAP II) in its hyperphosphorylated state to augment transcriptional elongation of specific genes (OTERO *et al.* 1999; GILBERT *et al.* 2004). Inconsistent with the positive role of the ELP complex in transcriptional

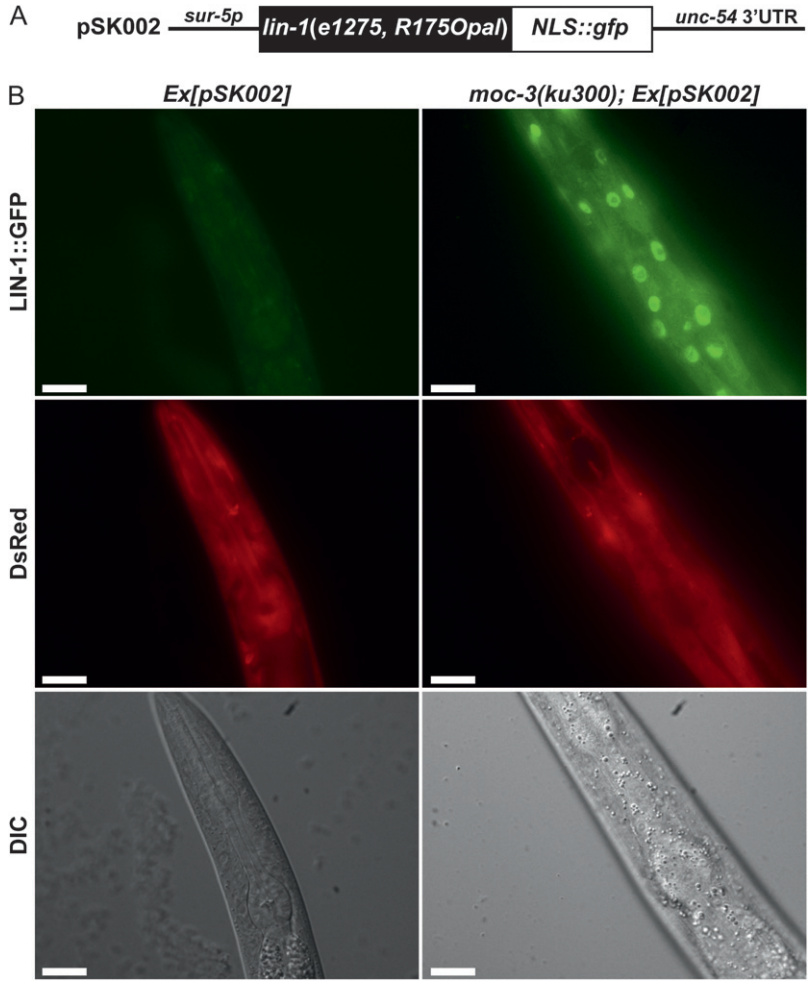

Figure 6.—A product of translational readthrough of *lin-1(e1275)* may be observed in the *moc-3(ku300)* background. (A) Schematic of the pSK002 construct. *lin-1(e1275)* cDNA was fused to GFP. NLS, nuclear localization signal. (B) The readthrough at R175Opal in *lin-1(e1275)* likely resulted in the expression of the LIN-1::GFP full-length protein in the nucleus. Shown here is the head region of representative L4 larvae. A *sur-5* promoter-driven DsRed construct was used as a marker for transgenic worms. Full genotypes are *Ex[pSK002], unc-119(ed3); him-5(e1467); Ex[pSK002], moc-3(ku300); Ex[pSK002], unc-119(ed3); moc-3(ku300); Ex[pSK002].* Bars, 20 μm.

elongation, the suppression of the Muv phenotype of *lin-1(e1275)* by *moc-3(lf)* and *dph-3(lf)* would implicate only a negative regulatory role of MOC-3 and DPH-3 on *lin-1* expression (Table 1). In addition, our data indicate that the regulation of *lin-1* by MOC-3 and DPH-3 is not likely to be transcriptional (Figure 4). Therefore, our genetic and molecular analyses of *moc-3*, *dph-3*, *urm-1*, and the genes encoding other ELP complex components suggest a function of the ELP complex unrelated to transcription elongation.

Recently, from the screening for novel proteasomal pathway components, several yeast mutants affecting *uba4*, *elp2*, and *elp6* exhibited defects in proteasomal function (Hoyt *et al.* 2008). This raised the possibility that the mutations of *moc-3* and the ELP complex led to the stabilization of the readthrough protein products from *lin-1(e1275)*. In the same study, however, a yeast *urm1* mutant did not show any proteasomal defect, whereas RNAi of *urm-1* in *C. elegans* suppressed the Muv phenotype of *lin-1(e1275)*, suggesting that the potential proteasomal function of Uba4p and the ELP complex may not affect the stability of the LIN-1(e1275)::GFP protein. In addition, as we mentioned above, Kti11p/DPH3 has another function, diphthamide synthesis, in yeast and humans (Liu and Leppla 2003; Liu *et al.* 2004). Diphthamide is a modified histidine residue in translation elongation factor 2 (eEF2) and might have a function in protein translation in eukaryotes, although its exact role remains elusive. Moreover, Uba4p and the ELP complex in yeast and mammals have not been shown to be involved in diphthamide synthesis. Therefore, further discussion may be suspended until we know more about the role of this modified histidine in protein translation. In theory, the suppression that we observed could also be caused by stabilization of the low level of full-length LIN-1 protein as a readthrough product from the *e1275* allele, and such stabilization could be the consequence of a novel response, such as a protein-folding response, to the production of the aberrant translation product. However, there is no evidence thus far to link Uba4p or the ELP complex to either of these possibilities. It is important to mention that the experimental evidence provided by a previous report (Esberg *et al.* 2006) raised the possibility that the Elongator complex is primarily involved in tRNA modification and that many of the other cellular defects observed in the mutants could be secondary effects caused by defects in translation.

Our data raise one intriguing question: What underlies the allele specificity of the suppression by mutating

TABLE 4

Overexpression of GFP-LIN-1(*e1275*) protein suppresses the Muv phenotype of *lin-1(n176)* in *moc-3(lf)* and *dph-3(lf)* backgrounds

Genotype	% multivulva (*n*)[a]
lin-1(n176) moc-3(tm3742)	100 (50)
lin-1(n176) dph-3(ku432)	100 (100)
kuIs76[b]	0 (100)
lin-1(n176)	100 (100)
lin-1(n176);kuIs76	95 (228)
lin-1(n176) moc-3(tm3742);kuIs76	21 (243)
lin-1(n176) dph-3(ku432);kuIs76	13 (47)

[a] Percentage of Muv animals at adult stage. *n*, the number of animals scored.

[b] The full genotype is *unc-119(ed3);him-5(e1467);kuIs76*.

the genes in the ELP complex? The *moc-3* and *dph-3* mutations did not suppress *unc-54(r308)*, *dpy-5(e61)*, or *lon-1(sp3)*, which also harbor premature opal stop codons (Table S4), indicating that *moc-3(lf)* and *dph-3 (lf)* are not general informational suppressors. Potentially, this difference may be due to the difference in the impact of disrupting the tRNA modification function in different tissues. However, this difference would not explain why *lin-1(n176)*, a strong loss-of-function allele of *lin-1* that has a premature opal stop codon, was not suppressed by *moc-3(lf)* or *dph-3(lf)* (Table 1). One possibility is that the *n176* transcript is subject to a stronger regulation by the nonsense-mediated mRNA decay (NMD) than is the *e1275* transcript, leading to a very low level of mRNA as the template for the readthrough activity. However, the fact that the opal stop codon of *n176(R225Opal)* is 50 codons after that of the *n1275 (R175Opal)* does not seem to favor this idea because the efficiency of NMD usually decreases when the position of premature stop codon is farther downstream (Longman *et al.* 2007). Supporting this notion, our qPCR data clearly showed that *lin-1(n176)* worms maintain a level of *lin-1* mRNA that is more than half that of wild type and similar to that of *lin-1(e1275)* (Figure S4). Alternatively, the difference between the two alleles could be due to the different sequence contexts flanking the stop codons.

Another issue is that we do not currently understand the spectrum of codon misreading caused by disrupting the tRNA modification function of the ELP complex. It has been shown that unmodified U_{34} of tRNA can bind to essentially any of the four nucleotides (Söll and RajBhandary 1995), leaving a possibility that the mutations in the ELP complex may cause misreading of a broad spectrum of different codons, including all three stop codons, even though we have identified misreading in only one opal codon *in vivo*. Additional genetic and biochemical analysis may be required to have a thorough understanding of the question.

It is important to point out that disrupting this complex has a more profound effect than just suppressing the *lin-1(e1275)* allele, as *dph-3* and *moc-3* mutants are associated with slow growth, partial lethality, and a weak high-incident-male (Him) phenotype. This is partly consistent with the previous data that a mutation affecting thiolation of tRNA causes a Him phenotype and genome instability (Dewez *et al.* 2008). These developmental defects may reflect codon misreading in many genes. Therefore, tRNA modification function of the ELP complex is expected to be one of the mechanisms that play important roles in accurate translation.

It is worth noting that *lin-1(e1275)* is a temperature-sensitive allele. The temperature sensitivity of *lin-1 (e1275)* is unique among *lin-1(lf)* alleles harboring premature stop codons (Beitel *et al.* 1995; Miley *et al.* 2004). In addition, the temperature sensitivity indicates that there may be a low level of translational readthrough bypassing the opal stop codon at the lower temperature. In other words, *moc-3(lf)* and *dph-3(lf)* may have facilitated the readthrough of the opal stop via aberrant tRNA modification in *lin-1(e1275)*, which is already prone to stop codon recognition failure. This is supported by the result that *lin-1(n176);kuIs76* showed a slightly suppressed Muv phenotype (95%), while *lin-1 (n176) moc-3(tm3742);kuIs76* and *lin-1(n176) dph-3 (ku432);kuIs76* displayed a substantially suppressed Muv phenotype (21% and 13%, respectively) (Table 4). Furthermore, we showed a potential readthrough protein product using the *lin-1(e1275)::gfp* transgene in the *moc-3(lf)* mutant (Figure 6). In that sense, the previous work on the exocytosis function of the ELP complex might need to be re-evaluated. It was reported that a null allele of *ELP1* could suppress the exocytosis defect of a mutant in the Rab guanine nucleotide exchange factor Sec2p (Rahl *et al.* 2005). Intriguingly, the authors of this report used one single mutant of the *sec2* gene, *sec2-59*, which has a temperature sensitivity and a premature opal stop codon that is similar to *lin-1 (e1275)* (Nair *et al.* 1990). This potential cause of allele-specific suppression has also been pointed out previously in another article (Svejstrup 2007).

In conclusion, we have identified the roles of two genes, *moc-3* and *dph-3*, involved in protein translation in *C. elegans* through isolating novel genetic suppressors of *lin-1(e1275)*. We provide evidence that the *e1275*-specific suppression by *moc-3(lf)* and *dph-3(lf)* is independent of the RAS/MAPK pathway and may involve the tRNA modification modules, including *urm-1* and the ELP complex. The phenotypes of these mutants (which demonstrate the suppression effect) likely reflect the fundamental functions of this complex in maintaining accurate translation. Further study would be required to elucidate how and to what extent this protein complex is involved in translation in *C. elegans*.

We thank S. Mitani for the *moc-3(tm3742)* strain and Haibo Liu, Amara Seng, and members of our laboratory for helpful discussion. We also thank Gunilla Jäger for performing the HPLC analysis of tRNA. Some nematode strains used in this work were provided by the Caenorhabditis Genetics Center, which is funded by the National Institutes of Health National Center for Research Resources. This work was supported by the Korea Research Foundation Grant funded by the Korean Government (Ministry of Education and Human Resources Development) (KRF-2006-352-C00062) to S.K., the Swedish Cancer Foundation (07 0637 to A.S.B.), the Swedish Science Research Council (621-2006-4269 to A.S.B.), the Bernhard and Signe Bäckström Foundation (223-438-07) to A.S.B., and the Howard Hughes Medical Institute, of which S.K. and W.J. were associates, A.K.S. is a lab manager, and M.H. is an investigator.

LITERATURE CITED

Beitel, G. J., S. G. Clark and H. R. Horvitz, 1990 Caenorhabditis elegans ras gene let-60 acts as a switch in the pathway of vulval induction. Nature **348:** 503–509.

Beitel, G. J., S. Tuck, I. Greenwald and H. R. Horvitz, 1995 The Caenorhabditis elegans gene lin-1 encodes an ETS-domain protein and defines a branch of the vulval induction pathway. Genes Dev. **9:** 3149–3162.

Brenner, S., 1974 The genetics of *Caenorhabditis elegans*. Genetics **77:** 71–94.

Burdine, R. D., C. S. Branda and M. J. Stern, 1998 EGL-17(FGF) expression coordinates the attraction of the migrating sex myoblasts with vulval induction in C. elegans. Development **125:** 1083–1093.

Chen, C., S. Tuck and A. S. Bystrom, 2009 Defects in tRNA modification associated with neurological and developmental dysfunctions in Caenorhabditis elegans elongator mutants. PLoS Genet. **5:** e1000561.

Cui, M., and M. Han, 2003 Cis regulatory requirements for vulval cell-specific expression of the Caenorhabditis elegans fibroblast growth factor gene egl-17. Dev. Biol. **257:** 104–116.

Dewez, M., F. Bauer, M. Dieu, M. Raes, J. Vandenhaute *et al.*, 2008 The conserved Wobble uridine tRNA thiolase Ctu1-Ctu2 is required to maintain genome integrity. Proc. Natl. Acad. Sci. USA **105:** 5459–5464.

Esberg, A., B. Huang, M. J. Johansson and A. S. Bystrom, 2006 Elevated levels of two tRNA species bypass the requirement for elongator complex in transcription and exocytosis. Mol. Cell **24:** 139–148.

Ferguson, E. L., and H. R. Horvitz, 1985 Identification and characterization of 22 genes that affect the vulval cell lineages of the nematode *Caenorhabditis elegans*. Genetics **110:** 17–72.

Fichtner, L., and R. Schaffrath, 2002 KTI11 and KTI13, Saccharomyces cerevisiae genes controlling sensitivity to G1 arrest induced by Kluyveromyces lactis zymocin. Mol. Microbiol. **44:** 865–875.

Fichtner, L., D. Jablonowski, A. Schierhorn, H. K. Kitamoto, M. J. Stark *et al.*, 2003 Elongator"s toxin-target (TOT) function is nuclear localization sequence dependent and suppressed by post-translational modification. Mol. Microbiol. **49:** 1297–1307.

Fire, A., S. Xu, M. K. Montgomery, S. A. Kostas, S. E. Driver *et al.*, 1998 Potent and specific genetic interference by double-stranded RNA in Caenorhabditis elegans. Nature **391:** 806–811.

Furukawa, K., N. Mizushima, T. Noda and Y. Ohsumi, 2000 A protein conjugation system in yeast with homology to biosynthetic enzyme reaction of prokaryotes. J. Biol. Chem. **275:** 7462–7465.

Gilbert, C., A. Kristjuhan, G. S. Winkler and J. Q. Svejstrup, 2004 Elongator interactions with nascent mRNA revealed by RNA immunoprecipitation. Mol. Cell **14:** 457–464.

Goehring, A. S., D. M. Rivers and G. F. Sprague, Jr., 2003a Attachment of the ubiquitin-related protein Urm1p to the antioxidant protein Ahp1p. Eukaryot. Cell **2:** 930–936.

Goehring, A. S., D. M. Rivers and G. F. Sprague, Jr., 2003b Urmylation: a ubiquitin-like pathway that functions during invasive growth and budding in yeast. Mol. Biol. Cell **14:** 4329–4341.

Gu, T., S. Orita and M. Han, 1998 Caenorhabditis elegans SUR-5, a novel but conserved protein, negatively regulates LET-60 Ras activity during vulval induction. Mol. Cell. Biol. **18:** 4556–4564.

Han, M., and P. W. Sternberg, 1990 let-60, a gene that specifies cell fates during C. elegans vulval induction, encodes a ras protein. Cell **63:** 921–931.

Hoyt, M. A., S. McDonough, S. A. Pimpl, H. Scheel, K. Hofmann *et al.*, 2008 A genetic screen for Saccharomyces cerevisiae mutants affecting proteasome function, using a ubiquitin-independent substrate. Yeast **25:** 199–217.

Huang, B., M. J. Johansson and A. S. Bystrom, 2005 An early step in wobble uridine tRNA modification requires the Elongator complex. RNA **11:** 424–436.

Huang, B., J. Lu and A. S. Bystrom, 2008 A genome-wide screen identifies genes required for formation of the wobble nucleoside 5-methoxycarbonylmethyl-2-thiouridine in Saccharomyces cerevisiae. RNA **14:** 2183–2194.

Kim, J. H., W. S. Lane and D. Reinberg, 2002 Human Elongator facilitates RNA polymerase II transcription through chromatin. Proc. Natl. Acad. Sci. USA **99:** 1241–1246.

Kornfeld, K., 1997 Vulval development in Caenorhabditis elegans. Trends Genet. **13:** 55–61.

Krogan, N. J., and J. F. Greenblatt, 2001 Characterization of a six-subunit holo-elongator complex required for the regulated expression of a group of genes in Saccharomyces cerevisiae. Mol. Cell. Biol. **21:** 8203–8212.

Leidel, S., P. G. Pedrioli, T. Bucher, R. Brost, M. Costanzo *et al.*, 2009 Ubiquitin-related modifier Urm1 acts as a sulphur carrier in thiolation of eukaryotic transfer RNA. Nature **458:** 228–232.

Liu, S., and S. H. Leppla, 2003 Retroviral insertional mutagenesis identifies a small protein required for synthesis of diphthamide, the target of bacterial ADP-ribosylating toxins. Mol. Cell **12:** 603–613.

Liu, S., G. T. Milne, J. G. Kuremsky, G. R. Fink and S. H. Leppla, 2004 Identification of the proteins required for biosynthesis of diphthamide, the target of bacterial ADP-ribosylating toxins on translation elongation factor 2. Mol. Cell. Biol. **24:** 9487–9497.

Liu, S., J. F. Wiggins, T. Sreenath, A. B. Kulkarni, J. M. Ward *et al.*, 2006 Dph3, a small protein required for diphthamide biosynthesis, is essential in mouse development. Mol. Cell. Biol. **26:** 3835–3841.

Longman, D., R. H. Plasterk, I. L. Johnstone and J. F. Caceres, 2007 Mechanistic insights and identification of two novel factors in the C. elegans NMD pathway. Genes Dev. **21:** 1075–1085.

Lu, J., B. Huang, A. Esberg, M. J. Johansson and A. S. Bystrom, 2005 The Kluyveromyces lactis gamma-toxin targets tRNA anticodons. RNA **11:** 1648–1654.

Miley, G. R., D. Fantz, D. Glossip, X. Lu, R. M. Saito *et al.*, 2004 Identification of residues of the *Caenorhabditis elegans* LIN-1 ETS domain that are necessary for DNA binding and regulation of vulval cell fates. Genetics **167:** 1697–1709.

Miller, L. M., M. E. Gallegos, B. A. Morisseau and S. K. Kim, 1993 lin-31, a Caenorhabditis elegans HNF-3/fork head transcription factor homolog, specifies three alternative cell fates in vulval development. Genes Dev. **7:** 933–947.

Nair, J., H. Muller, M. Peterson and P. Novick, 1990 Sec2 protein contains a coiled-coil domain essential for vesicular transport and a dispensable carboxy terminal domain. J. Cell Biol. **110:** 1897–1909.

Nakai, Y., M. Nakai and H. Hayashi, 2008 Thio-modification of yeast cytosolic tRNA requires a ubiquitin-related system that resembles bacterial sulfur transfer systems. J. Biol. Chem. **283:** 27469–27476.

Noma, A., Y. Sakaguchi and T. Suzuki, 2009 Mechanistic characterization of the sulfur-relay system for eukaryotic 2-thiouridine biogenesis at tRNA wobble positions. Nucleic Acids Res. **37:** 1335–1352.

Otero, G., J. Fellows, Y. Li, T. de Bizemont, A. M. Dirac *et al.*, 1999 Elongator, a multisubunit component of a novel RNA polymerase II holoenzyme for transcriptional elongation. Mol. Cell **3:** 109–118.

Rahl, P. B., C. Z. Chen and R. N. Collins, 2005 Elp1p, the yeast homolog of the FD disease syndrome protein, negatively regulates exocytosis independently of transcriptional elongation. Mol. Cell **17:** 841–853.

Rubio-Texeira, M., 2007 Urmylation controls Nil1p and Gln3p-dependent expression of nitrogen-catabolite repressed genes in Saccharomyces cerevisiae. FEBS Lett. **581:** 541–550.

Schlieker, C. D., A. G. Van der Veen, J. R. Damon, E. Spooner and H. L. Ploegh, 2008 A functional proteomics approach links the ubiquitin-related modifier Urm1 to a tRNA modification pathway. Proc. Natl. Acad. Sci. USA **105:** 18255–18260.

Schwarz, G., and R. R. Mendel, 2006 Molybdenum cofactor biosynthesis and molybdenum enzymes. Annu. Rev. Plant Biol. **57:** 623–647.

Söll, D., and U. Rajbhandary, 1995 *tRNA: Structure, Biosynthesis, and Function.* ASM Press, Washington, DC.

Sternberg, P. W., 2005 Vulval development (June 25, 2005), *WormBook*, ed. The *C. elegans* Research Community, WormBook, doi/10.1895/wormbook.1.6.1, http://www.wormbook.org.

Sternberg, P. W., and M. Han, 1998 Genetics of RAS signaling in C. elegans. Trends Genet. **14:** 466–472.

Sun, J., J. Zhang, F. Wu, C. Xu, S. Li *et al.*, 2005 Solution structure of Kti11p from Saccharomyces cerevisiae reveals a novel zinc-binding module. Biochemistry **44:** 8801–8809.

Sundaram, M., 2005 RTKRas/MAP kinase signaling (February 11, 2006), *WormBook*, ed. The *C. elegans* Research Community, WormBook, doi/10.1895/wormbook.1.80.1, http://www.wormbook.org.

Svejstrup, J. Q., 2007 Elongator complex: How many roles does it play? Curr. Opin. Cell Biol. **19:** 331–336.

Tan, P. B., M. R. Lackner and S. K. Kim, 1998 MAP kinase signaling specificity mediated by the LIN-1 Ets/LIN-31 WH transcription factor complex during C. elegans vulval induction. Cell **93:** 569–580.

Tiensuu, T., M. K. Larsen, E. Vernersson and S. Tuck, 2005 lin-1 has both positive and negative functions in specifying multiple cell fates induced by Ras/MAP kinase signaling in C. elegans. Dev. Biol. **286:** 338–351.

Winkler, G. S., T. G. Petrakis, S. Ethelberg, M. Tokunaga, H. Erdjument-Bromage *et al.*, 2001 RNA polymerase II elongator holoenzyme is composed of two discrete subcomplexes. J. Biol. Chem. **276:** 32743–32749.

Yandell, M. D., L. G. Edgar and W. B. Wood, 1994 Trimethylpsoralen induces small deletion mutations in Caenorhabditis elegans. Proc. Natl. Acad. Sci. USA **91:** 1381–1385.

Yochem, J., T. Gu and M. Han, 1998 A new marker for mosaic analysis in *Caenorhabditis elegans* indicates a fusion between hyp6 and hyp7, two major components of the hypodermis. Genetics **149:** 1323–1334.

Yoder, J. H., H. Chong, K. L. Guan and M. Han, 2004 Modulation of KSR activity in Caenorhabditis elegans by Zn ions, PAR-1 kinase and PP2A phosphatase. EMBO J. **23:** 111–119.

Communicating editor: D. I. Greenstein

GENETICS

Supporting Information
http://www.genetics.org/cgi/content/full/genetics.110.118406/DC1

Allele-Specific Suppressors of *lin-1(R175Opal)* Identify Functions of MOC-3 and DPH-3 in tRNA Modification Complexes in *Caenorhabditis elegans*

Sunhong Kim, Wade Johnson, Changchun Chen, Aileen K. Sewell, Anders S. Byström and Min Han

DOI: 10.1534/genetics.110.118406

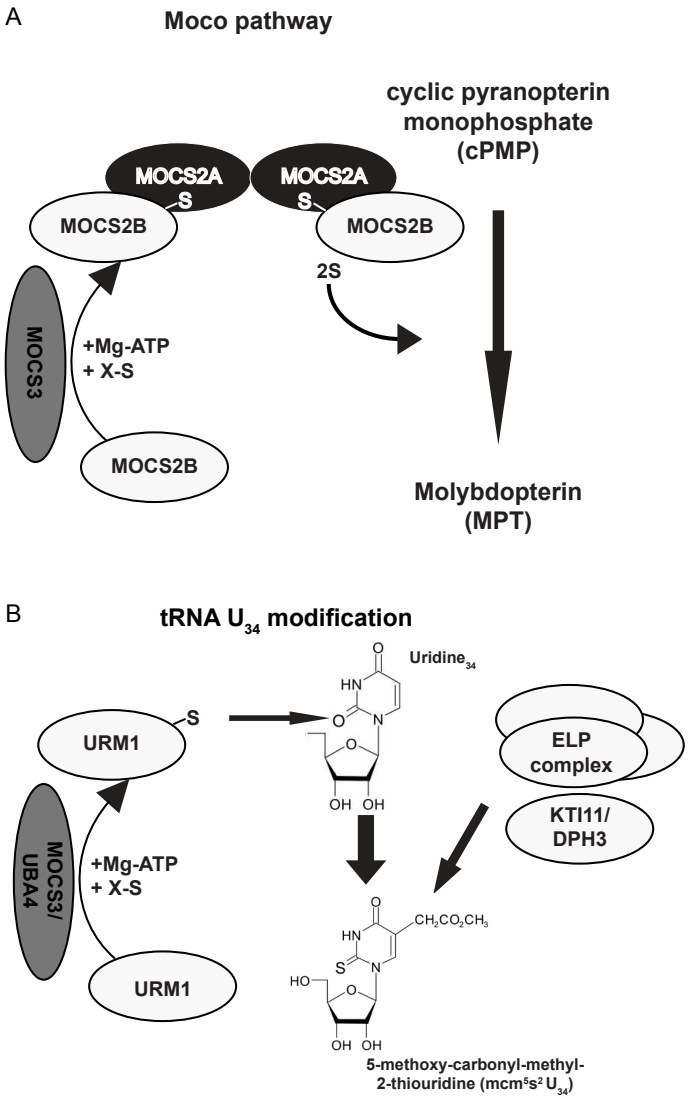

FIGURE S1.—(A) Schematic diagram depicting Moco synthesis pathway. (B) Illustration of uridine nucleotide modification by UBA4/URM1 module and ELP complex.

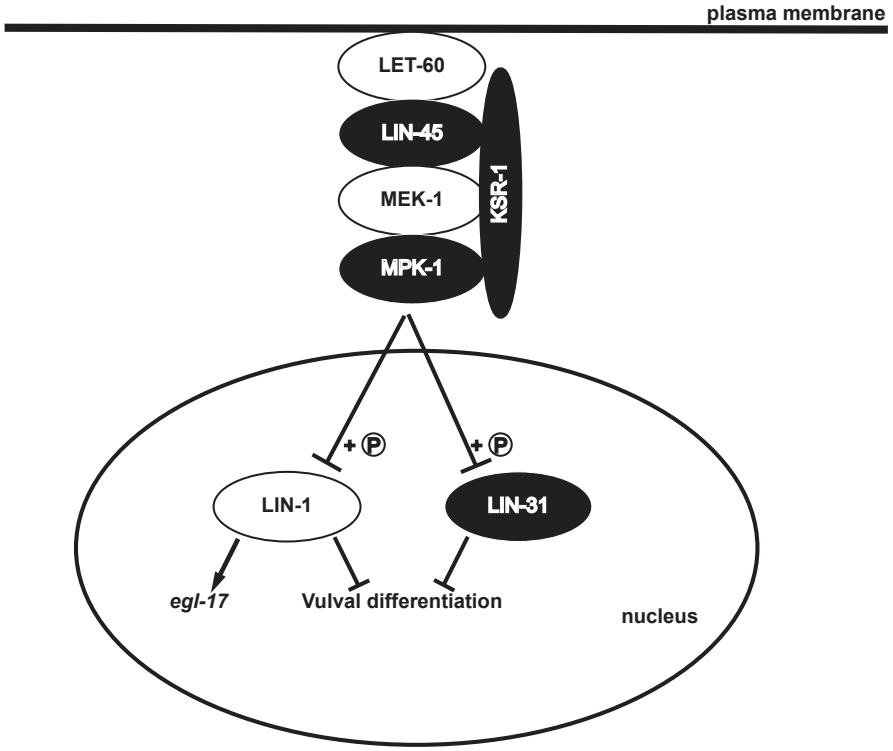

FIGURE S2.—Schematic diagram of Ras/MAPK pathway in the vulval development in *C. elegans*.

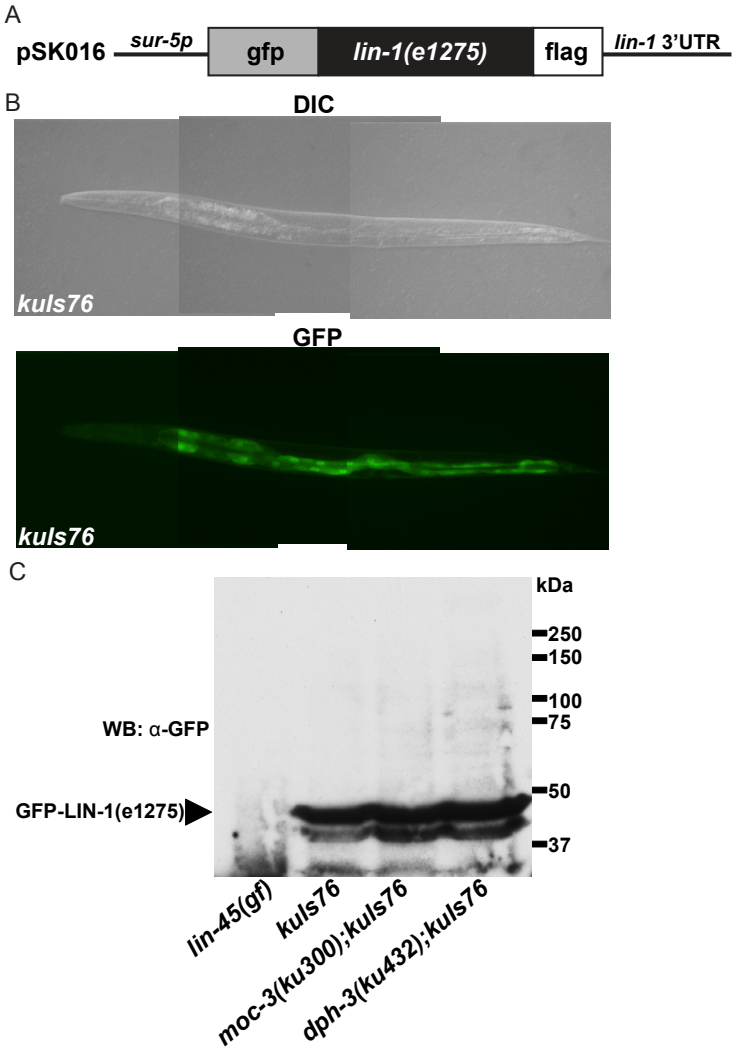

FIGURE S3.—Structure and expression of a *sur-5p::lin-1(e1275)::flag* fusion gene (*kuIs76*). A. Cartoon illustration of the structure of the fusion gene. B. Nomarski and GFP fluorescence of an adult worm expressing the fusion protein. C. Western blot of GFP-LIN-1(e1275) from the worm whole lysates. After the preparation of the worm lysates, proteins were detected by anti-GFP antibody via the standard enhanced chemiluminescence method. *lin-45(gf)* was used as a control because the *sur-5p::gfp* construct has been integrated with *lin-45(gf)* construct (YODER et al. 2004).

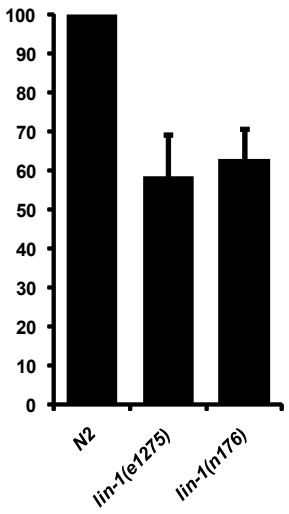

FIGURE S4.— Both alleles of *lin-1(e1275)* and *lin-1(n176)* have been subject to a similar level of nonsense-mediated decay. Bar diagram indicates the results of qRT-PCR analysis of mRNA levels of *lin-1* in strains listed. *rpl-26* was used as an internal control during the qRT-PCR experiments. Error bars indicates ±S.D. The difference between the means of *lin-1* mRNA level in *lin-1(e1275)* and *lin-1(n176)* mutants was not statistically significant ($p>0.05$).

TABLE S1

The *lin-1* gene *per se* is required for the suppression of the Muv phenotype of *lin-1(e1275)* by *moc-3(lf)* and *dph-3(lf)*

	%Multivulva (*n*)[a]			
	lin-1(e1275) moc-3(ku300)		*lin-1(e1275) dph-3(ku432)*	
GFP RNAi	3	(207)	1.7	(172)
lin-1 RNAi	14	(161)	17	(60)

[a] L4 worms of *lin-1(e1275) moc-3(ku300);rrf-3(pk1426)* and *lin-1(e1275) dph-3(ku432);rrf-3(pk1426)* were placed on RNAi plate and Muv phenotype of F1 were scored. *n*, the number of animals checked.

TABLE S2

ELP complex is likely to be in a linear pathway with *moc-3*, *dph-3*, and *urm-1*

	%Multivulva (*n*)[a]	
GFP RNAi	12	(126)
moc-3 RNAi	11	(131)
urm-1 RNAi	13	(152)
dph-3 RNAi	17	(99)

[a] L4 worms of *lin-1(e1275);elpc-3(ok2452)* were placed on RNAi plate and Muv phenotype of F1 were scored. *n*, the number of animals checked.

TABLE S3

***moc-3(lf)* and *dph-3(lf)* mutants are defective in wobble uridine tRNA modification**

Genotype	mcm^{5}s^{2}U[a]/Ψ[b]	s^{2}U[a]
N2	1[c]	-
lin-1(e1275)	0.68	-
moc-3(tm3742)	0	-
moc-3(ku300)	0	-
lin-1(e1275); *moc-3(ku300)*	0	-
dph-3(ku432)	0	+
lin-1(e1275); *dph-3(ku305)*	0	+

[a]Nucleosides mcm^{5}s^{2}U and s^{2}U stand for 5-methoxycarbonylmethyl-uridine and 2-thiouridine respectively. "+" and "-" indicate detection and non-detection of s^{2}U, respectively.

[b]Pseudouridine (Ψ) was used as an internal standard.

[c]The numbers given are the ratios of mcm^{5}s^{2}U and Ψ in total tRNA isolated from various mutants to the ratio in the wild type.

TABLE S4

***moc-3(tm3742)* and *dph-3(ku305)* did not suppress other premature opal stop codon mutants**

Genotype	%Phenotype (*n*)	
unc-54(r308)	100	(50)
unc-54(r308);dph-3(ku305)[a]	100	(50)
dpy-5(e61)	100	(100)
dpy-5(e61);moc-3(tm3742)	100	(100)
lon-1(sp3)	100	(100)
lon-1(sp3);moc-3(tm3742)	100	(100)

[a] The complete genotype is *unc-54(r308); lin-1(e1275) dph-3(ku305)*.